2D control of field-driven magnetic bubble movement using Dzyaloshinskii-Moriya interactions

Dorothée Petit,[1] Peter R. Seem,[2] Marine Tillette,[1] Rhodri Mansell,[1] and Russell P. Cowburn[1]
[1)] *Thin Film Magnetism group, Cavendish Laboratory, University of Cambridge, J. J. Thomson Avenue, Cambridge CB3 0HE, United Kingdom*
[2)] *Durham Magneto Optics Ltd, Church Farm, Gransden Road, Caxton, Cambridge CB23 3PL, United Kingdom*

The field-induced asymmetric growth of magnetic bubble domains in Pt/Co/Pt out-of-plane magnetized films with Dzyaloshinskii-Moriya interactions is used to control the lateral displacement of bubbles. We demonstrate experimentally that we can laterally translate bubbles away from their nucleation site by applying a series of alternating 3-dimensional field pulses with a controlled relative sign between the out-of-plane and in-plane components. Using magneto optical Kerr effect imaging the domain wall velocity as a function of applied field strength was measured from which the magnitude of the Dzyaloshinskii-Moriya interaction field was estimated.

Domain walls in magnetic thin films have been the object of intense research from the magnetism community for a number of years, due to their potential for spintronic devices, either as a possible route to low-power switching of magnetization[1,2] or as an intrinsic element to shift-register-based data storage architectures[3,4]. Ultrathin magnetic films with perpendicular anisotropy and Dzyaloshinskii-Moriya interactions (DMI)[5,6] are receiving renewed interest[7] for these applications because of recent developments in the understanding of DMI's role in controlling domain wall (DW) motion[8]: by stabilizing Néel DWs rather than Bloch DWs, the DMI is believed to be at the origin of the unusually high efficiency of DW motion in patterned strips[9–11], with obvious benefits to DW-based devices. Furthermore, DMI is at the origin of the stabilization of complex magnetic textures such as skyrmions[12,13]. The prospect of their existence in thin films opens up the possibility of using them as carriers for data storage devices[14].

In thin film systems, the DMI is due to the combination of strong spin-orbit interaction in the adjacent heavy metal non-magnetic layer and broken symmetry at the interface of the magnetic material[15]. The DMI couples two neighboring spins $\boldsymbol{S_1}$ and $\boldsymbol{S_2}$ via a neighboring atom with large spin-orbit interaction and takes the form $-\boldsymbol{D}\cdot\boldsymbol{S_1}\times\boldsymbol{S_2}$, with the DM vector $\boldsymbol{D}$ perpendicular to the unit vector joining $\boldsymbol{S_1}$ and $\boldsymbol{S_2}$ and in the interface plane. The DM interaction favors a perpendicular alignment between S_1 and S_2 such that both spins are in the plane perpendicular to the interface and perpendicular to $\boldsymbol{D}$, with the chirality of the $(\boldsymbol{S_1}, \boldsymbol{S_2})$ arrangement set by the sign of $\boldsymbol{D}$.

Recently, the DMI was shown in Pt/Co/Pt and Pt/Co/Ir/Pt systems to cause a sizable asymmetry in the velocity of out-of-plane (OOP) field-driven motion of DWs in the presence of an in-plane (IP) field, causing an asymmetry in the expansion of bubble domains[16–18]. This asymmetry was shown to depend on the direction of an IP magnetic field applied in conjunction to the OOP field responsible for the motion. Because of the DMI, the DW around the bubble is forced into the Néel-type with a well-defined chirality. The relative direction between the magnetization in the DW and the IP field is therefore also well-defined, and the DW velocity asymmetry was shown to be due to the IP field being parallel (increased velocity) or antiparallel (decreased velocity) to the magnetization inside the DW.

In this paper, we show that this effect can be extended to an arbitrary two-dimensional IP applied field[18]. Using magneto-optical Kerr effect (MOKE) microscopy[19] and a 3D magnetic field setup, we demonstrate 360-degree control of the direction of the asymmetric growth of bubbles in a similar Pt/Co/Pt multilayer. Furthermore, we show that we can use this effect to laterally translate a bubble domain in arbitrary directions. This work demonstrates control of the movement of bubbles without using patterned structures, opening up the possibility for arbitrary paths reconfigurable on-the-fly.

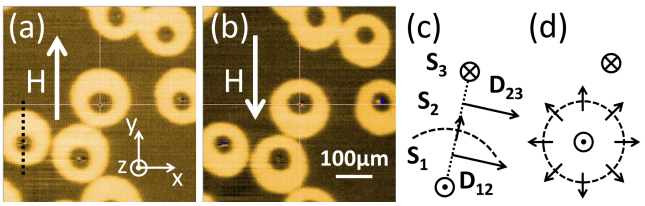

FIG. 1. (a), (b): Differential MOKE microscopy images of OOP field-driven expanding bubble domains with an IP bias field H of 1.4 kOe applied in the $+Y$ (a) and $-Y$ (b) directions, as indicated by the white arrows. The perpendicular component of the field pulse is 125 Oe. Inset: definition of the (X, Y, Z) directions. (c): illustration of the DMI in the case of a DW. (d): Circular upwards bubble domain and DW (dotted line). The arrows (both IP and pointing in and out of the plane) show the directions of the magnetization in the DW.

The sample studied here consists of a Ta (4 nm) / Pt (10 nm) / Co (0.8 nm) / Pt (3 nm) multilayer grown at room temperature by DC magnetron sputtering onto a Si substrate at an Ar pressure of 8×10^{-3} millibars. The MOKE microscopy setup allows the application of a 2D (X, Y) magnetic field using a quadrupole electro-

magnet. The sample holder has an integrated air-coil for the application of the perpendicular Z field. See figure 1 (a) for the definition of (X, Y, Z). Correct alignment of the quadrupole and the sample was ensured by confirming the symmetry of the effect upon application of a positive and a negative field in both the horizontal X direction and the vertical Y direction. Figure 1 (a) and (b) show images of bubble domains expanding under the influence of a 150 ms 125 Oe $+Z$-field applied in conjunction with an IP field of 1.4 kOe pointing in the $+Y$ (a) or the $-Y$ direction (b). The images are differential images obtained by subtracting the initial image with a bubble domain present (small dark disk) from the final image after the domain has expanded under the influence of the field pulse. Thus, bright regions show where the bubble domain has grown. It is clear that the DW expands asymmetrically: in the presence of a positive (negative) Y field the DW travels faster in the $+Y$ $(-Y)$ direction. This effect is attributed to the presence of DMI in the following way[16]. First, the effect of DMI on the morphology of a DW is illustrated in figure 1 (c), which shows three interacting spins across a DW. $\boldsymbol{S_1}$ $(\boldsymbol{S_3})$ is in the upward (downward) domain and $\boldsymbol{S_2}$ is in the DW itself. The DM vectors point in the plane of the interface and perpendicularly to the vector joining the two interacting spins[15]. For $\boldsymbol{S_1}$, $\boldsymbol{S_2}$ and $\boldsymbol{S_3}$ here, $\boldsymbol{D_{12}}$ and $\boldsymbol{D_{23}}$ point in the same direction, causing spins $\boldsymbol{S_1}$, $\boldsymbol{S_2}$ and $\boldsymbol{S_3}$ to form a Néel DW rather than a Bloch one, and to rotate around the relevant $\boldsymbol{D}$ with the same well-defined chirality. In the case of a DW enclosing a bubble domain, such as is illustrated figure 1 (d), the $\boldsymbol{D_{ij}}$ vectors at any point across the DW are tangential to the DW, causing the well-defined chirality to be preserved for the whole DW. The sign of $\boldsymbol{D}$ sets whether the Néel DW around an upward domain points inwards or outwards. While an IP field cannot act on the reversed domain itself, it breaks the rotational symmetry of the DW which encloses it, allowing the possibility of anisotropic expansion of the bubble. Within the creep regime formalism, it was found that the velocity dependence of the DW upon the IP field and DMI strength could be attributed to the dependence of the DW energy density upon the IP field and DMI strength[16]. More practically, the parts of the DWs which have their magnetization aligned with the IP field have a higher velocity than the parts of the DW which are anti-aligned. We note that all the bubbles present in the field of view are distorted in the same direction, confirming the homogeneity of the sign of the DMI vector.

We have used a series of images obtained when applying a Y bias field in order to extract the DW velocity as a function of the IP bias field strength for an OOP propagation field of 110 Oe. The velocity is extracted from differential images such as figure 1 (a) and (b), where the change between images is one field pulse of either 300 or 350 ms duration. The velocity of the DW is measured along the center of each bubble (dotted line in figure 1 (a)), and the results are averaged between all the bubbles present in the field of view. In figure 2 we show the domain wall velocity as a function of bias field. We measure the velocity of the top of the bubble, expanding in the $+Y$ direction, shown in red, and the bottom of the bubble, expanding in the $-Y$ direction, shown in blue. The in set in figure 2 shows this schematically. The data is symmetric around zero field, as expected, and the velocities show minima at around $\pm$ 500 Oe, corresponding to the IP applied field necessary to balance the DMI field and restore symmetry to the system. The DMI field is therefore of the order of 500 Oe in our multilayer. The sign agrees with previous work[16] for a similar system, and our simple estimate of the DMI field strength is of the same order of magnitude, confirming that we are observing the same effect.

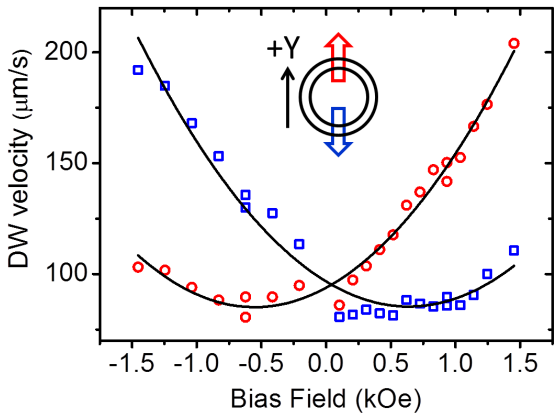

FIG. 2. DW velocity as a function of IP bias field for a $+Z$ propagation field value of 110 Oe. Red symbols give the velocity in the $+Y$ direction, blue symbols in the $-Y$ direction. The solid lines are a guide to the eye. Inset: Schematic of the measurement geometry.

Figure 3 (a)-(d) shows how the asymmetric growth of bubble domains can be controlled by applying a 2D IP field in arbitrary directions (shown by the white arrows in each image). In our experiment, the nucleation of bubbles is not controlled, rather we use naturally occurring defects to act as nucleation centers. After an initial negative saturation a $+Z$-field pulse is applied in the positive direction. The amplitude and duration of the field pulse ($\sim$125 Oe for $\sim$ 150 ms in this case) is adjusted so that only a few bubbles are activated within the $500 \times 500 \mu m^2$ field of view used for subsequent imaging. The initial domain is then expanded using a 75 Oe, 150 ms pulse and the Kerr image taken after this pulse is used as a background subtracted from subsequent images. Four 150 ms pulses at 125 Oe in $+Z$ are then applied with a 1 kOe in-plane field in the direction shown by the white arrow in the figure. Each image is binarized and normalized before being added to form the composite image. As expected, the effect seen in Figure 1 is seen for every field

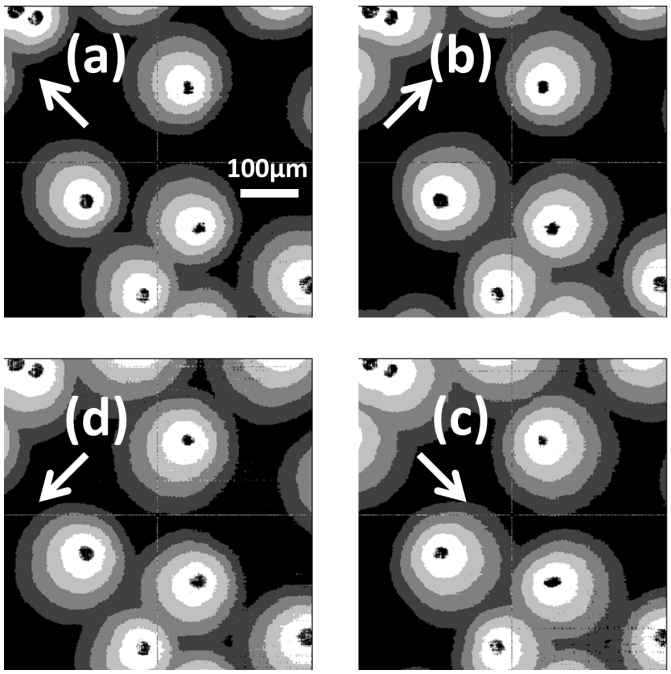

FIG. 3. (a-d): MOKE microscopy images of OOP field-driven expanding bubble domains with an IP bias field of 1 kOe applied in different directions, as indicated by the white arrows on each image. Each image is obtained by adding 4 consecutive Kerr images each corresponding to the application of a 150 ms long field pulse.

direction in the plane of the sample: the bubbles grow faster along the direction of the IP bias field.

The next step is to transform this controlled distortion of bubble domains into controlled movement. Figure 4 (a) is a schematic of the experiment performed in figure 1 (a), where an upward bubble (black) grows asymmetrically under the influence of an $+Z$ field and an IP bias field in the $+Y$ direction (red). The small black arrows indicate the magnetization direction in the DW. If both components of the field are reversed (figure 4 (b)), the bubble will shrink since the OOP component of the field is now opposite to the magnetization inside the bubble. Because the IP component of the field has also reversed, the side of the bubble which points in the same direction as the IP component of the field is now also reversed. The bottom of the bubble therefore shrinks faster than the upper part, causing the bubble to go from the initial black shape to the final blue shape. The final lateral position of the bubble in (b) is different from the initial position of the bubble in (a). The bubble was laterally translated in a controlled direction set by the IP component of the applied field.

The experimental realization of this is shown in figure 4 (c-s). Figure 4 (c-s) shows a series of MOKE images taken as symmetric pulses of alternating magnetic field (indicated at the bottom-right corner of each image) are sequentially applied in order to grow and shrink magnetic bubbles in an asymmetric fashion. First, a $-Z$ field pulse is applied for $\sim 1s$ in order to saturate the magnetization downwards - (c) is taken at remanence after negative saturation. The magnetization is uniformly pointing down. A $+Z$ field pulse of 110 Oe amplitude is then applied during 200 ms in order to nucleate bubble domains - (d) is then taken at remanence. Subsequently, 200 ms pulses of alternating fields with an Z component of 110 Oe and an IP component of 1.1 kOe at 36° clockwise from the X axis is applied. Figure 4 (e-s) are taken at remanence after each field pulse. The sign of the IP component of the field relative to the OOP component is chosen such that the top-left of the bubble moves faster than the bottom-right as the bubble grows while the bottom-right moves faster than the top-left as the bubble shrinks. This results in an inching movement of the bubbles towards the upper-left quadrant. This is clear when following the bubble highlighted in green for instance. In this particular experiment, the field used to propagate the bubble is strong enough, for the particular nucleation sites activated here, to nucleate new domains each time a pulse is applied. This is clear if again we follow the bubble highlighted in green. In (d) the just-nucleated bubble is centered on the nucleation site in the middle of the image. In (e), because of the IP bias field, it expands asymmetrically and grows faster in the $(-X, +Y)$ direction. In (f), a reverse field has been applied which is strong enough to nucleate a downward domain exactly where the initial upward domain was nucleated in (d) - highlighted in yellow. The resulting upward domain is the small crescent highlighted in green at the top left of the yellow disk. This pattern occurs for all bubbles within the field of view - three of these crescents are highlighted with a blue arrow. In (g), the field is reversed again in order to grow the bubbles asymmetrically towards the top-left of the image, which also nucleates a new upward domain under the yellow disk. The new yellow bubble and the expanded crescent merge. This pattern of nucleating new domains back and forth under the yellow disk while moving the initial green bubble towards the top-left of the image continues. From (o) onwards, the initial green bubble has moved far enough away from the nucleation center that it does not merge with the upward yellow bubble upon application of the upward field (o, q, s). The white cross in (o-s) is placed at the center of the green bubble in (o), emphasizing its displacement during the last three field pulses. The lateral bubble speed is half the difference in domain wall velocity for the opposite sides of the bubble in the bias field direction. The lateral bubble speed will, therefore, scale with the domain wall speed, which would allow much higher lateral bubble speed with greater magnitude pulse fields. For a 1.1 kOe in-plane bias field, the data in figure 2 gives a lateral speed of around $40\mu m/s$, which, for the 15 pulses of 200 ms length used in figure 4, leads us to expect travel of around $120\mu m$, similar to the $130\mu m$ travel observed.

A few points need commenting on. Firstly, the fact that only the green bubble appears to be able to es-

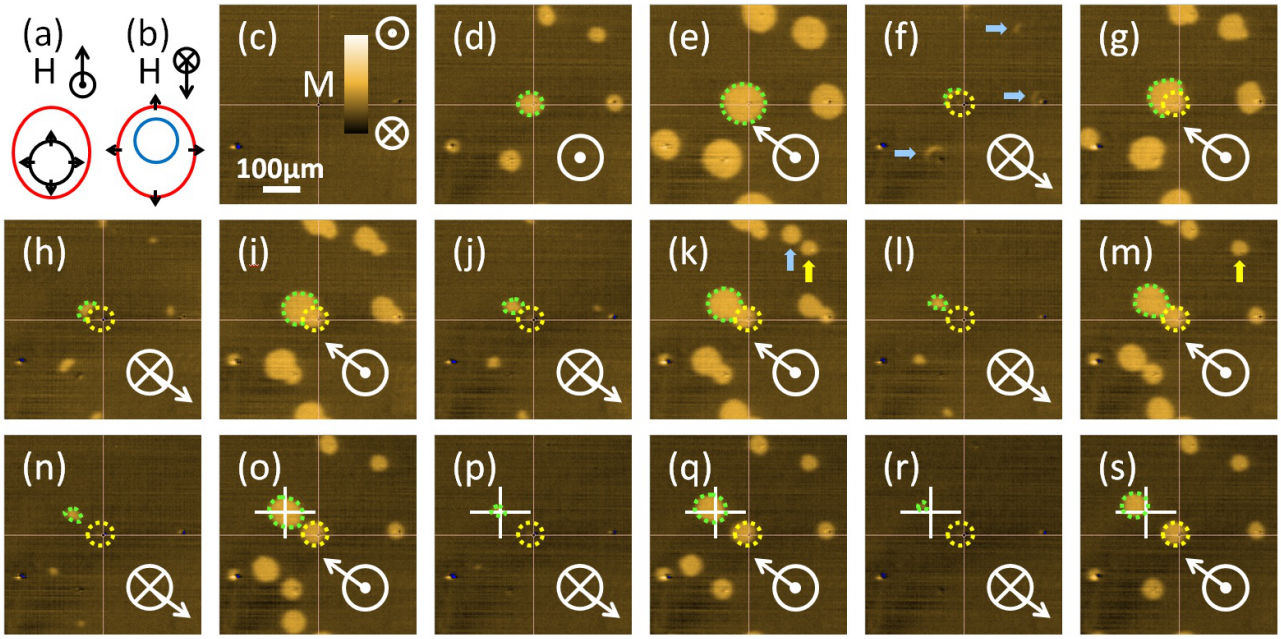

FIG. 4. (a), (b): Schematics showing the effect of applying alternating in-plane and out-of-plane magnetic fields. (c-s): Sequential series of MOKE images after pulses of alternating magnetic field (indicated at the bottom-right corner of each image) are applied. The OOP component of the applied field is 110 Oe, the IP component is 1.1 kOe.

cape the nucleation area to travel in the direction of the IP field. None of the subsequently-created yellow bubbles are moving. This is because the green bubble goes through an additional growing step (nucleation in (d) followed by growing in (e)), as compared to the yellow bubbles which only go through a nucleation / annihilation cycle. Secondly, the size of the bubbles decreases as they move, as shown by the green bubble, for instance, after it becomes independent from the nucleation center (compare (o), (q) and (s)). Some bubbles even annihilate in the process, see for instance the traveling bubble highlighted by a blue arrow in (k), which does not reappear at the subsequent growing step (m), where only its associated intermittent bubble is present at the corresponding nucleation site (yellow arrow in (k) and (m)). This behavior may be due to the effect of domain wall tension, which tends to increase the domain wall velocity of a shrinking bubble at small sizes[20].

In conclusion, we have used MOKE microscopy and a 3D magnetic field setup to demonstrate 360-degree control of the direction of the asymmetric growth of magnetic bubble domains in a Pt/Co/Pt multilayer with DMI. We have estimated the strength of the DMI field present in our film, and shown that we can use this asymmetric growth to move a bubble in arbitrary directions by applying alternating field pulses with both IP and OOP components of a defined relative sign. This work demonstrates control of the movement of bubbles without using patterned structures, opening up the possibility for arbitrary paths reconfigurable on-the-fly.

This work was supported by the European Community under the Seventh Framework Programme '3SPIN' (ERC contract 247368) and by EMRP JRP EXL04 SpinCal. The EMRP is jointly funded by the EMRP participating countries within EURAMET and the EU.

[1] A. Chanthbouala, R. Matsumoto, J. Grollier, V. Cros, A. Anane, A. Fert, A. V. Khvalkovskiy, K. A. Zvezdin, K. Nishimura, Y. Nagamine, H. Maehara, K. Tsunekawa, A. Fukushima and S. Yuasa, Nature Phys. 7, 626 (2011)
[2] D. A. Allwood, G. Xiong, C. C. Faulkner, D. Atkinson, D. Petit and R. P. Cowburn, Science 309, 1688 (2005)
[3] D. A. Allwood, G. Xiong, M. D. Cooke, C. C. Faulkner,D. Atkinson, N. Vernier and R. P. Cowburn, Science 206, 2003 (2002)
[4] S. S. P. Parkin, M. Hayashi and L. Thomas, Science 320, 190194 (2008)
[5] I. Dzialoshinski, J. Phys. Chem. Solids 4, 241 (1958)
[6] T. Moriya, Phys. Rev. Lett. 4, 228 (1960)
[7] A. Fert, Mater. Sci. Forum 59-60, 439 (1990)
[8] A. Thiaville, S. Rohart, É. Jué, V. Cros and A. Fert, Europhys. Lett. 100, 57002 (2012)
[9] I. M. Miron, T. Moore, H. Szambolics, L. D. Buda-Prejbeanu, S. Auffret, B. Rodmacq, S. Pizzini, J. Vogel, M. Bonfim, A. Schuhl and G. Gaudin, Nature Mater. 10, 419 (2011)
[10] S. Emori, U. Bauer, S.-M. Ahn, E. Martinez and G. S. D. Beach, Nature Mater. 12, 611 (2013)
[11] K.-S. Ryu, L. Thomas, S.-H. Yang and S. Parkin, Nature Nanotech. 8, 527 (2013)
[12] A. Bogdanov and A. Hubert, Journal of Magnetism and Magnetic Materials, 138, 255 (1994)
[13] N. Nagaosa and Y. Tokura, Nature Nanotechnology, 8, 899 (2013)
[14] J. Sampaio, V. Cros, S. Rohart, A. Thiaville and A. Fert, Nature Nano. 8, 839 (2013)
[15] A. Crépieux and C. Lacroix, J. Magn. Magn. Mat. 182, 341349 (1998)
[16] S.-G. Je, D.-H. Kim, S.-C. Yoo, B.-C. Min, K.-J. Lee and S.-B. Choe, Phys. Rev. B 88, 214401 (2013)

[17] A. Hrabec, N. A. Porter, A. Wells, M. J. Benitez Romero, G. Burnell, S. McVitie, D. McGrouther, T. A. Moore and C. H. Marrows, Phys. Rev. B 90, 020402(R) (2014)
[18] Y. P. Kabanov, Y. L. Iunin, V. I. Nikitenko, A. J. Shapiro, R. D. Shull, L. Y. Zhu, and C. L. Chien IEEE Transactions on Magnetics, 46, 2220 (2010)
[19] J.-H. Lee, R. Mansell, D. Petit, A Fernández-Pacheco, R. Lavrijsen and R.P. Cowburn, SPIN 3, 1340013 (2013)
[20] K.-W. Moon, J.-C. Lee, S.-G. Je, K.-S. Lee, K.-H. Shin and S.-B. Choe, Applied Physics Express, 4, 043004, (2011)